

Accelerated Publications

Mutagenesis of Acidic Residues in the Oxygenase Domain of Inducible Nitric-Oxide Synthase Identifies a Glutamate Involved in Arginine Binding[†]

Ratan Gachhui,[‡] Dipak K. Ghosh,[‡] Chaoqun Wu,[‡] John Parkinson,[§] Brian R. Crane,^{||} and Dennis J. Stuehr^{*,‡}

Department of Immunology, The Cleveland Clinic Research Institute, Cleveland, Ohio 44195, Berlex Biosciences, Richmond, California 94804, and Department of Molecular Biology, Scripps Research Institute, La Jolla, California 92037

Received February 13, 1997; Revised Manuscript Received March 20, 1997[®]

ABSTRACT: The oxygenase domain of the mouse cytokine-inducible nitric-oxide synthase (iNOSox, amino acids 1–498) binds heme, tetrahydrobiopterin, and the substrate Arg and is the domain responsible for catalyzing nitric oxide synthesis and maintaining the enzyme's active dimeric structure. To further understand iNOSox structure–function, we carried out alanine point mutagenesis on 15 conserved acidic residues located within a region of iNOSox (amino acids 352–473) that shares sequence homology with the pterin-binding module in dihydrofolate reductases and may be important for iNOSox subunit dimerization and/or Arg binding. Five point mutants were identical or nearly identical to wild-type, while 10 exhibited a range of defects that included low heme content (2), heme ligand instability (2), defective dimerization (2), and poor Arg and/or tetrahydrobiopterin binding (4). Mutations that caused defective tetrahydrobiopterin binding were also associated with other defects. In contrast, two mutants (E371A and D376A) exhibited an exclusive defect in Arg binding. These mutants were dimeric, indicating that dimerization of iNOSox in *Escherichia coli* does not require Arg. In one case (E371A), the defect in Arg binding was absolute, as assessed by spectral perturbation, radioligand binding, and catalytic studies. We conclude that mutagenesis of conserved acidic residues within this region of iNOSox can lead to exclusive defects in dimerization and in Arg binding. Modeling considerations predict that the E371 carboxylate may participate in Arg binding by interacting with its guanidine moiety.

Nitric oxide (NO)¹ has emerged as an important signal and effector molecule in the immune, nervous and cardiovascular systems (Kroncke et al., 1995; Garthwaite &

Boulton, 1995; Umans & Levi, 1995). Three isoforms of NO synthase (NOS) have been characterized that generate NO from L-arginine (Arg) in a stepwise reaction that generates *N*^ω-hydroxy-Arg (NOHA) as an intermediate [for reviews, see Griffith and Stuehr (1995) and Marletta (1993)].

[†] This work was supported by National Institute of Health Grant CA53914 to D.J.S. D.J.S. is an Established Investigator of the American Heart Association.

^{*} Author to whom correspondence should be addressed: Immunology NN-1, The Cleveland Clinic Foundation, 9500 Euclid Avenue, Cleveland, OH 44195, Phone: 216-445-6950. Fax: 216-444-9329. E-mail: stuehrd@cesmtp.ccf.org.

[‡] Cleveland Clinic Research Institute.

[§] Berlex Biosciences.

^{||} Scripps Research Institute.

[®] Abstract published in *Advance ACS Abstracts*, April 15, 1997.

¹ Abbreviations: Arg, L-arginine; CaM, calmodulin; DHFR, dihydrofolate reductase; DTT, dithiothreitol; EPPS, 4-(2-hydroxyethyl)-1-piperazinepropanesulfonic acid; FAD, flavin adenine dinucleotide; FMN, flavin mononucleotide; H₄B, (6*R*,6*S*)-2-amino-4-hydroxy-6-(L-erythro-1,2-dihydroxypropyl)-5,6,7,8-tetrahydropteridine; NNA, *N*^ω-nitro-L-arginine; NOHA, *N*^ω-hydroxy-L-arginine; NO, nitric oxide; iNOS, inducible NO synthase; iNOSox, inducible NO synthase oxygenase domain.

All NOSs are homodimers in their active form, and each subunit exhibits a bidomain structure comprised of an N-terminal oxygenase domain and a C-terminal reductase domain (Bredt et al., 1991). The oxygenase domain binds heme, tetrahydrobiopterin (H_4B), and Arg; contains determinants for subunit dimeric interaction; and is the site where the chemistry of NO synthesis takes place (Chen et al., 1996; Ghosh & Stuehr, 1995; Sheta et al., 1994; McMillan & Masters, 1995; Venema et al., 1997; Ghosh et al., 1996). The reductase domain binds FMN, FAD, calmodulin (CaM), and NADPH; is monomeric; and is responsible for transferring electrons from NADPH to the oxygenase domain during NO synthesis (Ghosh & Stuehr, 1995; McMillan & Masters, 1995; Gachhui et al., 1996). The individual domains can fold and function independently and when mixed together catalyze NO synthesis (Chen et al., 1996; Ghosh et al., 1995). Dimerization of NOS oxygenase domains is important because it allows flavin-mediated heme iron reduction to occur (Siddhanta et al., 1996), which in turn may enable the enzyme to activate dioxygen for NO synthesis (Griffith & Stuehr, 1995; Marletta, 1993).

Although sequence analysis and mutagenesis have identified amino acids that are involved in binding NADPH, FAD, FMN, CaM, and heme iron in NOS (Bredt et al., 1991; McMillan & Masters, 1995; Chen et al., 1994; Xie et al., 1994, 1996; Richards & Marletta, 1994; Venema et al., 1996), a similar understanding has not been reached regarding Arg and H_4B binding within the oxygenase domain. Two groups have noted that a conserved ~160 amino acid stretch of the oxygenase domain shares sequence homology with the pterin-binding module of dihydrofolate reductases [46% homology; the mouse inducible NOS (iNOS) DHFR module] (Nishimura et al., 1995) and with a region contained in the aromatic amino acid hydroxylases that is proposed to bind H_4B (Cho et al., 1995). However, when the DHFR module of rat neuronal NOS was expressed as a fusion protein, it did not bind labeled H_4B but instead appeared capable of binding the Arg analog N^w -nitroarginine (NNA) (Nishimura et al., 1995). In a separate study (Cho et al., 1995), point mutagenesis of two conserved uncharged residues within the DHFR module of iNOS generated mutants that could not form a homodimer. Unfortunately, the impact of these two mutations on H_4B binding could not be assessed because even wild-type iNOS monomers appear incapable of binding H_4B (Baek et al., 1993; Abu-Soud et al., 1995). On the other hand, point mutagenesis of a conserved cysteine located in an unrelated region of the NOS oxygenase domain did generate a dimeric protein whose only defect appeared to be a lower affinity toward H_4B (Chen et al., 1995). Thus, these results suggest that residues outside the NOS DHFR module may influence H_4B binding, while residues within the module may participate in dimerization and/or Arg interaction with NOS.

To address this issue within the context of our structure–function studies of iNOS (Ghosh et al., 1996; Siddhanta et al., 1996), we individually mutated 15 conserved acidic residues in the iNOS DHFR module to determine whether any might be involved in binding the basic guanidino or α -carbon amino groups of Arg. The results identify residues that impact on a range of NOS properties, including Arg and H_4B binding, heme properties, and dimerization, and also identify an amino acid selectively involved in Arg binding.

MATERIALS AND METHODS

Materials. [3H]NNA (55 Ci/mmol) was from Amersham. All other chemicals were obtained from sources as indicated in the text or as published previously (Gachhui et al., 1996; Baek et al., 1993).

Molecular Biology. Wild-type and mutant iNOSox (amino acids 1–498) with a His₆ tag attached to the C-terminus of the protein were overexpressed in *Escherichia coli* strain BL21(DE3) using a modified PCWori vector and purified as described (Siddhanta et al., 1996; Wu et al., 1996). Restriction digestions, cloning, bacterial growth and transformation, and isolation of DNA fragments were performed using standard procedures (Sambrook et al., 1989). Site-directed mutagenesis was done using the Altered Sites II in vitro Mutagenesis kit from Promega. Wild-type iNOSox DNA was cut from PCWori with *Cla*I, blunt-ended using the Klenow reaction, and cloned into the *Sma*I site of the pALTER-1 mutagenesis vector. Incorporated mutations were confirmed by DNA sequencing at the Cleveland Clinic core facility. DNA's containing the desired mutations were cloned into the *Nde*I/*Sall*I sites of the PCWori vector and transformed into *E. coli* BL21(DE3) for protein expression.

Oligonucleotides used to construct site-directed mutants in the iNOSox DHFR module were synthesized by Life technologies. Mutations and corresponding oligonucleotides were as follows: E352A, pATGCTACTGGCGGTGGGTG-GC; E357A, pGGTGGCCTCGCATTCCCAGCC; E371A, pATGGGCACCGCGATTGGAGTT; D376A, pGGAGT-TCGAGCCTTCTGTGAC; D379A, pGACTTCTGTGCCA-CACAGCGC; E387A, pAACATCTGGCGGAAGTGGGC; E388A, pATCCTGGAGGCGATGGGCCGA; E396A, pGATGGGCCTGGCGACCCACAC; D406A, pCTCTG-GAAAGCCCCGGCTGTC; E411A, pGCTGTACAGGC-GATCAATGTG; D429A, pACCATCATGGCCACCA-CACA; E435A, pACAGCCTCAGCGTCCTTCATG; E444A, pATGCAGAATGCGTACCGGGCC; D454A, pTGCCCG-GCAGCCTGGATTGG; E473A, pTTCCACCAGGCGAT-GTTGAAC.

Expression and Purification of Wild-Type and Mutant iNOSox. Transformed bacteria were grown at 37 °C in 250 mL of terrific broth supplemented with 125 mg/L ampicillin to an OD₆₀₀ of 1.0. Protein expression was induced with 1 mM isopropyl β -D-thiogalactoside, and the cultures were supplemented with 0.4 mM δ -aminolevulinic acid. After further growth at 25 °C for 48 h, the cells were harvested and resuspended in buffer A (40 mM EPPS, pH 7.6 with 10% glycerol and 0.25 M NaCl) containing 0.5 μ g/mL each of leupeptin, pepstatin, and phenylmethanesulfonyl fluoride (PMSF). Cells were lysed by freeze–thawing three times in liquid nitrogen followed by sonication for three 25 s pulses with a 1 min rest on ice between pulses, using a medium probe Sonicator Cell Disruptor (Model W-220F, Heat Systems, Ultrasonics, Inc.). The cell lysate was centrifuged at 4 °C for 30 min, and the cell-free supernatant was kept at –70 °C. An aliquot was removed to determine the P450 heme protein content (Siddhanta et al., 1996).

The cell-free supernatant was loaded onto a Ni²⁺-nitrilotriacetic acid Sepharose CL4B column that had been charged with 50 mM NiSO₄ and equilibrated with buffer A containing 1 mM PMSF. The column was washed with 15 mL of column buffer and 15 mL of column buffer containing 40 mM imidazole. The iNOSox protein was eluted with a

Rat nNOS	553	-----WFK	DLGLKWYGLP	AVSNMLLEIG	GLEFSACPFS	GWYMGTEIGV	595
Mouse iNOS	332	-----WFQ	ELGLKWYALP	AVANMLLEVG	GLEFPACPFN	GWYMGTEIGV	374
Bovine eNOS	324	-----WFA	ALGLRWYALP	AVSNMLLEIG	GLEFSAAPFS	GWYMSTEIGT	366
Human DHFR				D15	E30		
Rat nNOS	596	RDYCDNSRYN	ILEEVAKKMD	LDMRKTSSLW	KDQALVEINI	AVLYSFQSDK	645
Mouse iNOS	375	RDYCDTQRYN	ILEEVGRRMG	LETHTLASLW	KDRAVTEINV	AVLHSFQKQN	424
Bovine eNOS	367	RNLCDPHRYN	ILEDVAVCMD	LDTRTTSSLW	KDKAAVEINL	AVLHSFQLAK	416
Human DHFR			E44				
Rat nNOS	646	VTIVDHSAT	ESFIKHMENE	YRCRGGCPAD	WVWIVPPMSG	SITPVFHQEM	695
Mouse iNOS	425	VTIMDHTAS	ESFMKHMONE	YRARGGCPAD	WIWLVPPVSG	SITPVFHQEM	474
Bovine eNOS	417	VTIVDHAAT	VSFMKHLDNA	QKARGGCPAD	WAWIVPPISG	SLTPVFHQEM	466
Human DHFR			E101	D110			
Rat nNOS	696	LNYRLTPSFE	YQDPWNTHV	WKGNTGTPK	RRAIG		730
Mouse iNOS	475	LNYVLSPFYY	YQIEPWKTHI	WQNEKLRP-R	RREI-		507
Bovine eNOS	467	VNYILSPAFR	YQDPWKGS	TKGAGITR-K	KTFKE		500

FIGURE 1: Conserved acidic residues within the DHFR modules of three NOS isoforms. The iNOSox amino acid sequence representing the DHFR module is aligned with homologous sequences in rat neuronal NOS (nNOS) and bovine endothelial NOS (eNOS). Acidic residues that are conserved among the NOSs are underlined. Those that align with corresponding acidic residues in human DHFR based on the alignment of Nishimura et al. (1995) are indicated. Residues in iNOSox that were mutated to alanine are in bold.

gradient of 40 to 300 mM imidazole. Fractions containing P450 heme protein were pooled, adjusted to 1 mM DTT, and concentrated using a centrprep-30. Samples were dialyzed against 100 volumes of column buffer containing 1 mM DTT, no NaCl, and with or without 10 μ M H₄B at 4 °C. After three changes of buffer, the protein was checked for P450 heme content and purity by SDS-PAGE, and stored at -70 °C.

UV-Visible Spectroscopy. Spectral data was recorded on a Hitachi U3110 spectrophotometer in the presence or absence of H₄B and Arg. Scans of the dithionite-reduced CO-bound proteins were taken in 40 mM EPPS, pH 7.6, containing 10% glycerol, 1 mM DTT, 3 mM Arg, and 10 μ M H₄B. The ferrous-CO adduct absorbing at 444 nm was used to quantitate the heme protein content using an extinction coefficient of 74 mM⁻¹ cm⁻¹ ($A_{444}-A_{500}$). (Stuehr & Ikeda-Saito, 1992).

Spectral analysis of H₄B binding was done at room temperature with protein samples diluted in 40 mM EPPS, pH 7.6, containing 10% glycerol and 1 mM DTT. Spectra were recorded after adding 10, 100, and 300 μ M H₄B. In some cases, the time course of H₄B binding to iNOSox was monitored at 400 nm at 30 °C. Analysis of Arg binding was done using perturbation difference spectroscopy essentially as described (Ghosh et al., 1996; McMillan & Masters, 1993). Protein samples were diluted to ~3 μ M in buffer containing 10% glycerol, 1 mM DTT, 300 μ M H₄B, and 0.4 mM imidazole to promote formation of fully low-spin heme prior to the titration. Spectra were recorded 30 min after each addition of Arg. The final sample volume change was kept less than 5%. Difference spectra were generated by subtracting the spectrum obtained without Arg from each subsequent spectrum using Spectra Calc software (Galactic Industries Corp.). Spectral binding constants for Arg were determined from double reciprocal plots of the difference in the respective peak to trough absorbances versus the Arg concentration.

Gel Filtration Analysis. Dimer and monomer content of iNOSox proteins was estimated by chromatography on a Pharmacia Superdex-200 HR size-exclusion column equilibrated with 40 mM EPPS, pH 7.4, 10% glycerol, 0.25 M NaCl, 0.5 mM DTT, and in some cases 3 mM Arg and 10 μ M H₄B (Ghosh et al., 1996). The molecular weight of the

protein peaks were estimated relative to protein molecular weight standards.

Product Formation from NOHA. Catalysis of nitrite production from NOHA and H₂O₂ by iNOSox or mutants was assayed in 96-well microplates at 37 °C as previously described (Pufahl et al., 1995) with modifications. Assays (100 μ L of final volume) contained 100 mM Hepes, pH 7.5, 150 nM heme protein, 1 mM NOHA, 0.5 mM DTT, 27 mM H₂O₂, 10 units/mL SOD, 50 μ g/mL bovine serum albumin, and variable concentrations of H₄B. Reactions were started by adding H₂O₂ and stopped by adding catalase (1300 units). Griess reagent (100 μ L) was then added, and the assay plate was read at 550 nm in a Thermomax plate reader. Nitrite production was quantitated based on NaNO₂ standards.

[³H]NNA Binding. [³H]NNA binding was studied in 96-well immobilon-P (MAIP N45) filtration plates using a Millipore MultiScreen Assay System as previously described (Liu & Gross, 1995; Klatt et al., 1994). Wild-type iNOSox (36 pmol) was used in each 0.1 mL assay also containing 40 mM EPPS, pH 7.6, 1 mM DTT, 150 000 cpm (~2.5 pmol) of [³H]NNA in the presence or absence of H₄B (10 or 300 μ M). To determine K_d values for NNA, the iNOSox samples were incubated in triplicate for 30 min at 27 °C with increasing concentrations of unlabeled NNA (0–100 μ M). The reaction was stopped by rapid filtration using a Millipore vacuum manifold. Wells were washed once under vacuum with 0.2 mL of assay buffer. After air-drying, counts bound on the membrane filter discs were determined by liquid scintillation counting. Nonspecific binding was determined by including 5 mM NNA in a set of incubations, and the count thus obtained was subtracted from each experimental total binding value to obtain specific binding.

RESULTS

Alanine screening mutagenesis of 15 conserved acidic residues located in the DHFR module of iNOSox was done according to the diagram in Figure 1. Mutant protein expression was generally similar to wild-type iNOSox which averaged approximately 10–40 mg of heme protein per liter of culture. There were two exceptions (E352A and D406A) which consistently yielded very low expression of what

Table 1: Characterization of Mutants

protein	defect	% dimer ^a	H ₄ B (μ M) ^b	activity EC ₅₀ of H ₄ B (μ M)	K _s (μ M) L-Arg ^c	NNA binding ^d
wild-type	none	95	10	3	28 \pm 4	2.3 \pm 0.2
E357A	none	95	10	3	52 \pm 2	2.5 \pm 0.2
E371A	Arg binding	95	10	nd	nd	nd
D376A	Arg binding	95	10	7	<i>e</i>	0.3 \pm 0.1
D379A	H ₄ B and/or Arg binding	70	100	nd	<i>f</i>	0.2 \pm 0.1
E387A	none	90	10	3	112 \pm 12	1.9 \pm 0.2
E388A	none	90	10	3	45 \pm 5	2.0 \pm 0.2
E396A	none	90	10	4	50 \pm 2	1.8 \pm 0.2
E411A	dimerization	40	10	3	62 \pm 2	2.2 \pm 0.2
D429A	heme, H ₄ B, and/or Arg binding	60	nd	nd	nd	nd
E435A	none	90	10	3	130 \pm 5	2.3 \pm 0.2
E444A	heme, H ₄ B, and/or Arg binding	60	nd	nd	nd	nd
D454A	H ₄ B and/or Arg binding	70	100	20	225 \pm 20	0.5 \pm 0.1
E473A	dimerization H ₄ B and/or Arg binding	25	nd	nd	nd	0.1 \pm 0.1

^a With 10 μ M H₄B and 3 mM Arg. ^b Lowest tested concentration of H₄B (10, 100, and 300 μ M) required to displace DTT as sixth ligand, determined spectrally. ^c The concentration of Arg required for half-maximal displacement of imidazole (0.4 mM), in the presence of 300 μ M H₄B. Values represent the mean \pm SD for three determinations. ^d Picomoles bound. Wells contained 36 pmol of P450 heme protein, 2.3 pmol of [³H]NNA and 100 pmol of NNA. One picomole of bound NNA represented 1500 cpm. Nonspecific bound counts averaged 706 \pm 134 cpm per well. Values represent the mean \pm SD for three to six samples each. nd = not detectable. ^e D376A showed binding between 10 and 100 mM Arg without imidazole. ^f D379A exhibited moderate binding after overnight incubation with 100 mM Arg at 4 °C.

appeared to be heme-deficient, degraded iNOSox. These mutants could not be further analyzed. All other point mutants were purified and compared to wild-type regarding their heme content and properties, monomer–dimer ratio, Arg and H₄B binding, and catalysis of NOHA oxidation (Table 1 and Figure 3).

Of 13 mutants tested, 11 had heme contents and spectral properties similar to wild-type, displaying a Soret peak near 417 in the absence of Arg and H₄B that shifted to 444 nm upon reduction and CO binding (data not shown). This indicated that their heme iron is ligated to a cysteine thiolate as in wild-type. However, the mutants D429A and E444A upon dithionite reduction and CO binding gave mixed Soret peaks, of which 80% was positioned at 420 nm and 20% was at 444 nm (data not shown). This suggests that mutagenesis of D429 and E444 perturbs heme interaction with the protein and destabilizes the iron–thiol ligation in the reduced, CO-bound form.

Gel filtration analysis in the presence or absence of H₄B showed that 11 of the 13 mutants were primarily dimeric, while two (E411A and E473A) were predominately monomeric (Table 1). Thus, other than these two sites, mutagenesis of conserved acidic residues in the DHFR module did not destabilize the dimeric structure of iNOSox.

H₄B binding to iNOSox can displace DTT as a sixth heme iron ligand, and this process can be observed spectrally as a shift from a split to a single Soret absorbance centered at 400 nm (Ghosh et al., 1996). We thus utilized spectral change to compare mutant affinities toward H₄B. As shown in Table 1, most of the mutants displayed a normal response compared to wild-type in that 10 μ M H₄B was sufficient to displace the DTT ligand. Two mutants (D379A and D454A) required 10-fold higher concentrations of H₄B to achieve the same result. For mutants D429A, E444A, and E473A, H₄B did not displace the DTT ligand even after a 90 min incubation with 300 μ M H₄B at 30 °C.

Spectral perturbation analysis of Arg binding was carried out in the presence of 400 μ M imidazole and 300 μ M H₄B. Table 1 lists the concentrations of Arg which displaced 50% of the imidazole from the heme iron of each mutant. A range of responses were obtained. Four mutants (E357A, E388A,

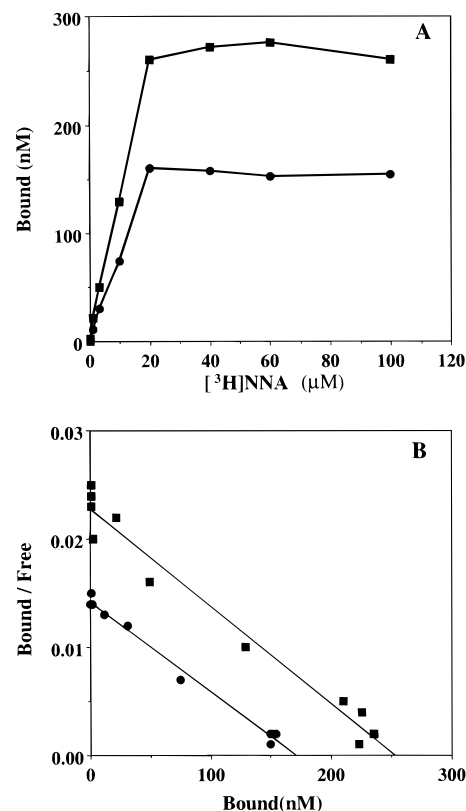


FIGURE 2: Binding of the Arg analog [³H]NNA to iNOSox. Panel A shows binding of [³H]NNA as a function of NNA concentration in the presence or absence of 0.3 mM H₄B. Panel B depicts the Scatchard plots obtained from the saturation binding curves of panel A. Bound [³H]NNA was plotted against bound/free where free is the molar concentration of [³H]NNA calculated from the difference between total and bound [³H]NNA. The plots were generated from three independent binding experiments each.

E396A, and E411A) required only slightly greater concentrations of Arg (within a factor of 3) when compared to wild-type, while two mutants (E387A and E435A) required 4–5 times the Arg concentration, and one mutant (D454A) 8 times the concentration. We were unable to determine a K_s for Arg by this method for six mutants. Of these, three that possessed normal heme properties were further investigated

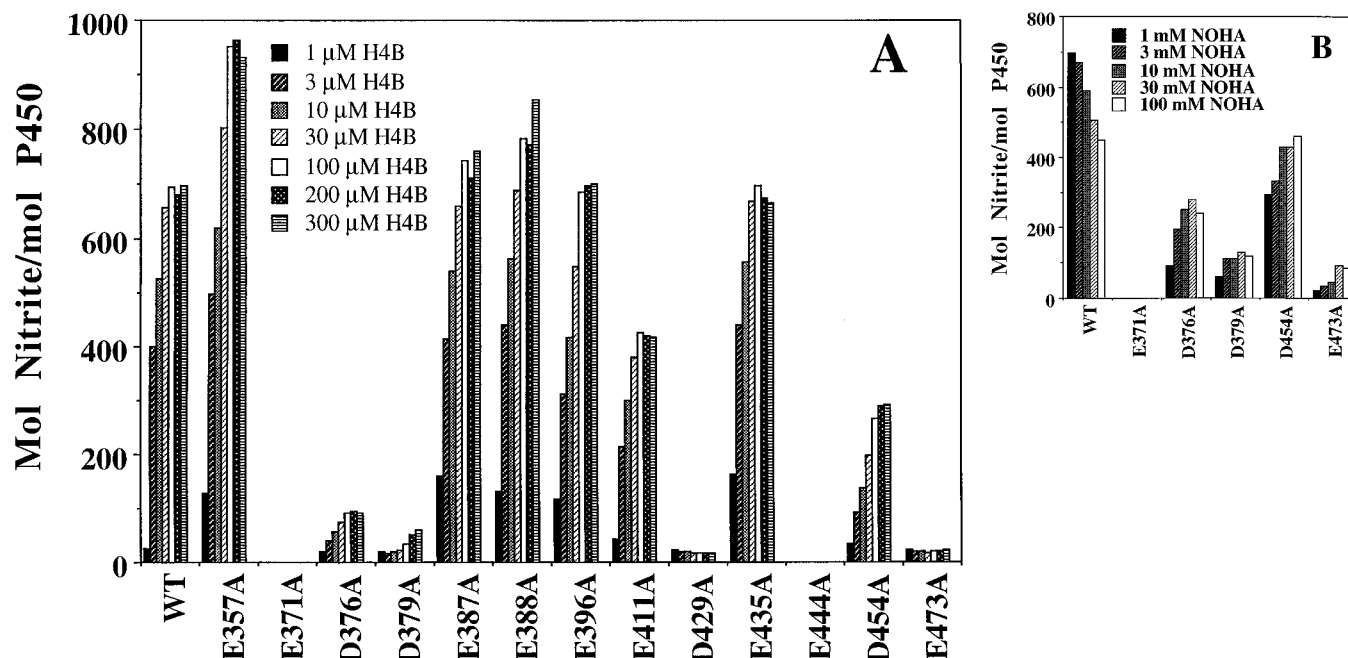


FIGURE 3: Catalytic activity of mutants as a function of H₄B or NOHA concentration. Panels A and B show product nitrite formed from NOHA in a 10 min H₂O₂-dependent assay at 37 °C. Assays were performed as indicated in Materials and Methods and contained 150 nM heme protein, the indicated concentrations of H₄B and NOHA, and were initiated by adding H₂O₂. The values shown are the average of three independent experiments. Panel A: assays contained 1 mM NOHA and various concentrations of H₄B (1–300 μ M). Panel B: assays contained a fixed concentration of H₄B (300 μ M) and various NOHA concentrations (1–100 mM).

regarding substrate interaction in the absence of imidazole. E371A did not undergo spectral perturbation even after overnight incubation with 100 mM Arg and also did not respond spectrally to a number of Arg or guanidine analogs (NOHA, NNA, aminoguanidine, and *S*-ethylisothiourea; data not shown), some of which bind much more tightly to iNOS than Arg itself (Sennequier & Stuehr, 1996; Garvey et al., 1994). In contrast, D376A did undergo a spectral change indicative of binding in response to 10 or 100 mM Arg, while D379A required overnight incubation with 100 mM Arg to achieve a positive response.

To further examine substrate interaction with the mutants, we carried out filter binding studies using [³H]NNA as a radioligand. Figure 2, panel A, shows specific binding of [³H]NNA to wild-type iNOS α as a function of NNA concentration in the presence or absence of 300 μ M H₄B. Specific binding under both conditions was concentration dependent and saturable. The Scatchard plot (Figure 2, panel B) suggests a single binding site for NNA with *K_d* of 10.1–11.4 μ M. Inclusion of H₄B in the binding assay only enhanced the binding capacity without affecting the *K_d*.

Specific binding of [³H]NNA to the mutants was quantitated in the presence of 300 μ M H₄B and 1 μ M cold NNA under otherwise identical conditions. As noted in Table 1, E357A, E387A, E388A, E396A, E411A, and E435A all maintained quantities of specifically bound NNA similar to wild-type iNOS α , whereas D376A, D379A, and E473A displayed low but detectable binding. Only E371A, D429A, and E444A showed no detectable binding by this assay. In general, results from the binding study were consistent with the spectral analysis of Arg binding.

We next examined each mutant's ability to catalyze product formation from NOHA in a 10 min H₂O₂-promoted reaction (Pufahl et al., 1995). Figure 3, panel A, shows the specific activities of each mutant when assayed in the presence of 1 mM NOHA and various H₄B concentrations

(1–300 μ M). Under these conditions, we failed to detect any activity for E371A or E444A, while four mutants (D376A, D379A, D429A, and E473A) showed a range of lower activities and five mutants (E357A, E387A, E388A, E396A, and E435A) showed activity essentially identical to wild-type. EC₅₀ values for H₄B derived from Figure 3, panel A, are listed in Table 1. The lower activity of E411A may possibly be due to its predominantly monomeric structure, while lower activity of D454A may reflect higher concentration requirements for both Arg and H₄B.

Certain mutants that displayed less than maximal activity (D376A and D454A), very little activity (D379A and E473A), or no activity (E371A) were reassayed in the presence of higher H₄B or NOHA concentrations. As shown in Figure 3, panel B, increasing the NOHA concentration to 100 mM (all with 300 μ M H₄B) led to concentration-dependent increases in activity for D376A, D454A, D379A, and E473A, but not E371A, which remained totally inactive. In the case of D376A or D454A, activities obtained at higher NOHA concentrations approached or equaled that of wild-type iNOS α , whereas the activities of D379A and E473A achieved maxima that were still below wild-type. One mutant displaying poor H₄B binding (D379A) was reassayed in the presence of 1 mM NOHA and greater H₄B concentrations. Its activity was still increasing even at 1 mM H₄B (data not shown).

DISCUSSION

Our current objective was to identify conserved acidic residues in the DHFR module of iNOS that may be involved in subunit interaction and/or H₄B and Arg binding. Individual mutagenesis of 15 acidic residues within this module had little discernible effect in only five cases and otherwise produced a wide range of iNOS α phenotypes (Table 1). These include proteins with defective heme incorporation,

heme properties, H₄B binding, Arg binding, and subunit dimeric interaction. This clearly indicates multiple roles for the conserved acidic residues within this region of iNOSox. It is remarkable that of seven mutants found defective in H₄B or Arg binding, six maintain a primarily dimeric structure and thus are among the first examples of NOS mutants that possess defects toward H₄B or Arg binding in the absence of defective dimerization.² Thus, Arg or H₄B may not be required for iNOSox to dimerize when being overexpressed in *E. coli*.

Two mutations (D429A and E444A) adversely affected the iNOS heme environment as evidenced by their forming unstable ferrous–CO complexes. These mutants also exhibited little or no capacity to bind Arg and H₄B or catalyze product formation from NOHA in the H₂O₂-supported reaction, in spite of their maintaining considerable dimeric structure. Thus, mutation of these two acidic residues may cause changes in iNOSox structure that affect both the heme environment and cofactor or substrate binding.

Only two mutants were partially (E411A) or substantially (E473A) defective in forming a dimer. Poor dimerization appeared to be the only defect of E411A, because it otherwise exhibited normal H₄B and Arg binding affinity and was catalytically active in full proportion to its dimeric content. In contrast, catalytic activity by E473A was lower than that predicted based on its monomer–dimer ratio, consistent with its also displaying poor affinity toward H₄B and Arg.

Two mutants (D379A and D454A) were defective in binding both H₄B and Arg but otherwise displayed normal heme properties and dimer content. D454A exhibited a similar decrease in affinity toward both molecules, whereas D379A was primarily defective in binding Arg. However, when either mutant was provided with higher concentrations of NOHA, their catalytic activities in the H₂O₂-supported reaction approached that of wild-type iNOSox, implying that their defect was primarily in binding and not in catalytic function.

Two mutations located within five residues of each other (E371A and D376A) were selectively defective in binding Arg. However, D376A was found to bind trace levels of radiolabeled NNA and exhibited a small amount of catalytic activity that plateaued at high concentrations of NOHA. This indicates its Arg binding defect was not absolute, and the mutation may also cause a defect in catalytic function. In contrast, the E371A mutant was completely unable to bind Arg or NNA based on our radioisotope, spectral, and catalytic assays for substrate interaction. Its failure to bind Arg extended to substrate analogs that display higher affinity toward iNOS, such as thiocitrulline and *S*-ethylisothiourea (Garvey et al., 1994). Thus, mutagenesis of conserved anionic residue E371 in iNOS appears to cause a selective defect in Arg binding that is also absolute.

Given that E371 is a highly conserved acidic residue among the NOS DHFR modules and DHFR enzymes (Nishimura et al., 1995; Figure 1), we examined what role the homologous residue E30 plays in human DHFR regarding interactions between the protein and the pterin ring of dihydrofolate. As shown in the left side of Figure 4, the

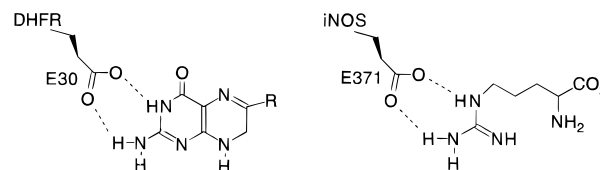


FIGURE 4: Possible role for conserved iNOS residue E371. The left drawing depicts an interaction that occurs in human DHFR between its E30 carboxylate and the pterin ring “guanidino” nitrogens of dihydrofolate, according to crystal structure data (Davies et al., 1990). The side chain of dihydrofolate (R) was omitted for clarity. The right drawing depicts a similar interaction that could occur between the homologous E371 carboxylate of iNOS and two guanidino nitrogens of Arg.

crystal structure indicates that the E30 carboxylate forms hydrogen bonds with two “guanidine” nitrogens of the pterin ring. On the basis of our current data, we speculate that the E371 carboxylate could perform a similar function in iNOS by hydrogen bonding with two of the three guanidino nitrogens of Arg³ (Figure 4, right side). Indeed, a similar interaction between a protein carboxylate and two guanidino nitrogens has been shown to hold Arg within the active site of arginase (Kanyo et al., 1996). In iNOS, Arg appears to derive little binding energy from interactions of its α -amino group with the iNOS protein (Garvey et al., 1994; Sennequier & Stuehr, 1996). Consequently, loss of a carboxylate–Arg interaction as depicted in Figure 4 would be expected to greatly diminish or eliminate Arg binding to the protein, consistent with what is observed upon mutagenesis of E371 to an uncharged residue.⁴ Thus, iNOS may provide a remarkable example of functional conservation within the DHFR module, in which a common acidic residue interacts with guanidino nitrogens present in two structurally distinct substrates.

Although our current results identify an acidic residue in the iNOS DHFR module whose mutation may exclusively prevent Arg binding, it is clear that other acidic (this study) and neutral (Cho et al., 1995) residues within the module impact on distinct aspects of iNOS structure–function, including subunit dimerization, heme content and properties, and H₄B interaction. Such multifaceted utilization of the DHFR module differentiates iNOS from DHFRs, which utilize the module to bind substrate and NADPH (Bystroff et al., 1990). It will be interesting to examine the basis of this difference and determine how the iNOS DHFR module functions in the larger context of oxygenase domain structure and catalysis.

NOTE ADDED IN PROOF

While this paper was in review, a paper appeared [Chen, P.-F., et al. (1997) *J. Biol. Chem.* 272, 6114–6118] that showed mutagenesis of the analogous residue in human endothelial NOS (E361) selectively abolished Arg binding.

³ Protein carboxylate–Arg interactions that involve one bridging (N^{α}) and one terminal (N^{ω}) nitrogen of Arg (as drawn for iNOS in Figure 4) are much more prevalent than those involving two terminal Arg nitrogens (Singh et al., 1987). A similar interaction for iNOS is proposed based on data with Arg analogs that show carbon substitution of one N^{ω} nitrogen is tolerated whereas substitution of the N^{β} nitrogen uniformly abolishes high binding affinity (Kerwin et al., 1995).

⁴ A related mutant in which an anionic residue is maintained at this site (E371D) can bind Arg and exhibits catalytic activity (R. Gachhui and D. J. Stuehr, unpublished results).

² The only other example may be point mutation of a conserved cysteine (C99 in endothelial NOS) that causes decreased H₄B affinity (Chen et al., 1995).

ACKNOWLEDGMENT

We thank Pam Clark for technical assistance and Drs. E. Getzoff and J. Tainer for helpful discussion.

REFERENCES

- Abu-Soud, H. M., Loftus, M., & Stuehr, D. J. (1995) *Biochemistry* 34, 11167–11175.
- Baek, K. J., Thiel, B. A., Lucas, S., & Stuehr, D. J. (1993) *J. Biol. Chem.* 268, 21120–21129.
- Bredt, D. S., Hwang, P. M., Glatt, C. E., Lowenstein, C., Reed, R. R., & Snyder, S. H. (1991) *Nature* 351, 714–718.
- Bystroff, C., Oakley, S. J., & Kraut, J. (1990) *Biochemistry* 29, 3263–3277.
- Chen, P.-F., Tsai, A.-L., & Wu, K. K. (1994) *J. Biol. Chem.* 269, 25062–25066.
- Chen, P.-F., Tsai, A. L., & Wu, K. K. (1995) *Biochem. Biophys. Res. Commun.* 215, 1119–1129.
- Chen, P.-F., Tsai, A.-L., Berka, V., & Wu, K. K. (1996) *J. Biol. Chem.* 271, 14631–14635.
- Cho, H. J., Martin, E., Xie, Q.-w., Sassa, S., & Nathan, C. (1995) *Proc. Natl. Acad. Sci. U.S.A.* 92, 11514–11518.
- Davies, J. F., Delcamp T. J., Prendergast, N. J., Ashford, V. A., & Freisheim, J. H. (1990) *Biochemistry* 29, 9467–9479.
- Gachhui, R., Presta, P. A., Bentley, D. F., Abu-Soud, H. M., McArthur, R., Brudvig, G., Ghosh, D. K., & Stuehr, D. J. (1996) *J. Biol. Chem.* 271, 20594–25602.
- Garthwaite, J., & Boulton, C. L. (1995) *Annu. Rev. Physiol.* 57, 683–706.
- Garvey, E. P., Oplinger, J. A., Tanoury, G. J., Sherman, P. A., Fowler, M., Marshall, S., Harmon, M. F., Paith, J. E., & Furfine, E. S. (1994) *J. Biol. Chem.* 269, 26669–26676.
- Ghosh, D. K., & Stuehr, D. J. (1995) *Biochemistry* 34, 801–807.
- Ghosh, D. K., Abu-Soud, H. M., & Stuehr, D. J. (1995) *Biochemistry* 34, 11316–11320.
- Ghosh, D. K., Abu-Soud, H. M., & Stuehr, D. J. (1996) *Biochemistry* 35, 1444–1449.
- Griffith, O. W., & Stuehr, D. J. (1995) *Annu. Rev. Physiol.* 57, 707–736.
- Kanyo, Z. F., Scolnick, L. R., Ash, D. E., & Christianson, D. W. (1996) *Nature* 383, 554–557.
- Kerwin, J. F., Jr., Lancaster, J. R., Jr., & Feldman, P. L. (1995) *J. Med. Chem.* 38, 4342–4362.
- Klatt, P., Schmidt, K., Brunner, F., & Mayer, B. (1994) *J. Biol. Chem.* 269, 1674–1680.
- Kroncke, K. D., Fehsel, K., & Kolb-Bachofen, V. (1995) *Biol. Chem. Hoppe-Seyler* 376, 327–343.
- Liu, Q., & Gross, S. S. (1995) *Methods Enzymol.* 268, 311–325.
- Marletta, M. A. (1993) *J. Biol. Chem.* 268, 12231–12234.
- McMillan, K., & Masters, B. S. S. (1993) *Biochemistry* 32, 9875–9890.
- McMillan, K., & Masters, B. S. S. (1995) *Biochemistry* 34, 3586–3693.
- Nishimura, J. S., Martasek, P., McMillan, K., Salerno, J. C., Liu, Q., Gross, S. S., & Masters, B. S. S. (1995) *Biochem. Biophys. Res. Commun.* 210, 288–294.
- Pufahl, R. A., Wishnok, J. S., & Marletta, M. A. (1995) *Biochemistry* 34, 1930–1941.
- Richards, M. K., & Marletta, M. A. (1994) *Biochemistry* 33, 14723–14732.
- Sambrook, J., Fritsch, E. F., & Maniatis, T. (1989) *Molecular Cloning: A Laboratory Manual*, Cold Spring Harbor Laboratory Press, Plainview, NY.
- Sennequier, N., & Stuehr, D. J. (1996) *Biochemistry* 35, 5883–5892.
- Sheta, E. A., McMillan, K., & Masters, B. S. S. (1994) *J. Biol. Chem.* 269, 15147–15153.
- Siddhanta, U., Wu, C., Abu-Soud, H. M., Zhang, I., Ghosh, D. K., & Stuehr, D. J. (1996) *J. Biol. Chem.* 271, 7309–7312.
- Singh, J., Thornton, J. M., Snarey, M., & Campbell, S. F. (1987) *FEBS Lett.* 224, 161–171.
- Stuehr, D. J., & Ikeda-Saito, M. (1992) *J. Biol. Chem.* 267, 20547–20550.
- Umans, J. G., & Levi, R. (1995) *Annu. Rev. Physiol.* 57, 771–790.
- Venema, R. C., Sayegh, H. S., Kent, J. D., & Harrison, D. G. (1996) *J. Biol. Chem.* 271, 6435–6440.
- Venema, R. C., Ju, H., Zou, R., Ryan, J. W., & Venema, V. J. (1997) *J. Biol. Chem.* 272, 1276–1282.
- Wu, C., Zhang, J., Abu-Soud, H. M., Ghosh, D. K., & Stuehr, D. J. (1996) *Biochem. Biophys. Res. Commun.* 222, 439–444.
- Xie, Q.-w., Cho, H. J., Kashiwabara, Y., Baum, M., Weidner, J. R., Elliston, K., Mumford, R., & Nathan, C. (1994) *J. Biol. Chem.* 269, 28500–28505.
- Xie, Q.-w., Leung, M., Fuortes, M., Sassa, S., & Nathan, C. (1996) *Proc. Natl. Acad. Sci. U.S.A.* 93, 4891–4896.

BI970331X